

CARBON MONOXIDE AND SEA SURFACE RETRIEVAL ALGORITHM FOR MICROMAPS MISSIONS

Patrick E. Hopkins,^{a,*} Vickie S. Connors,^b Margaret Pippin,^b Henry G. Reichle,^b and Robert J. Ribando^a

Abstract

The scientific goal of the Micro Measurement of Air Pollution from Satellites (μ MAPS) project is to measure carbon monoxide (CO) mixing ratios in the middle troposphere from an airborne platform. Recent work has focused the development of a data processing algorithm to determine precise scientific total column amounts of carbon monoxide from μ MAPS flights onboard Proteus in 2004. In this paper, the development of the current data reduction procedure for CO retrieval is presented. The μ MAPS calibration data and the various radiative transfer models, both vital steps in CO retrieval, are discussed. The retrieval algorithm is applied to the July 22, 2004 flight (which occurred during the INTEX-NA campaign) over the Atlantic Ocean off the coast of North America. Sea surface temperature and preliminary CO total column and mixing ratio calculations from this flight are presented and compared with retrievals from DACOM and AIRS – other CO-measuring instruments.

I. Introduction

Carbon monoxide (CO) is a colorless, odorless gas found in the troposphere that is produced by both natural and anthropogenic activities. Understanding the sources, sinks, transport, and distribution of CO is critical to understanding the overall chemistry of the troposphere. The major natural source of CO is the oxidation of hydrocarbons, such as methane (CH_4), in both the northern and southern hemispheres. The major anthropogenic sources are technological activities, such as the combustion of fossil fuels in the northern hemisphere and the burning of biomass primarily in the tropics.¹ These sources of atmospheric CO now appear to be of comparable magnitude.² A detailed discussion of the sources of CO is found in the references.³

The principle sink for CO is its oxidation by the hydroxyl radical (OH) in the troposphere. The hydroxyl radical is produced naturally in a two step process involving the photolysis of ozone (O_3) and a reaction of $\text{O}(^1\text{D})$ with water vapor (H_2O). This radical is the major oxidizer of all reduced species in the atmosphere. The increase in world wide agricultural and human technological activity has caused a significant increase in CO concentration in the atmosphere. Because CO accounts for the destruction of about 80% of OH in the troposphere, and because OH is the principal oxidizer of all reduced species, the emissions of CO can have a significant effect on the chemistry of the troposphere.⁴ For example, OH is a principal oxidizer of CH_4 , which is radiatively active, and other higher hydrocarbons, which are chemically active. An increase in CO concentration leads to the destruction of OH in the atmosphere, which in turn leads to increased levels of radiatively and chemically active gasses that contribute to changes in the planetary radiation balance.

Carbon monoxide was first detected in the atmosphere using solar spectroscopic observations.⁵ The presence of the gas was confirmed by direct

measurement techniques with average mixing ratios on the order of 100 ppbv in rural areas and up to 3 times higher in urban areas.¹ The current understanding of the concentration of CO in the atmosphere is very well studied and documented.⁶ In the 1960's, the National Aeronautics and Space Administration (NASA) sponsored studies to determine the feasibility of measuring the distribution of pollutant gasses from an orbiting satellite. These studies showed that CO would be measurable through the use of the gas filter cell radiometer (GFCR) technique.⁷

A successful GFCR project was NASA's Measurement of Air Pollution from Satellites (MAPS) experiment. The measurement of near-global distribution of CO was the primary science goal of MAPS. This experiment was flown on the Space Shuttle four times during November 1981, October 1984, and April and October 1994. The four Space Shuttle based MAPS missions lasted up to 10 days and covered a latitude range of up to 57° inclination orbit. The results from these test flights are presented in several works.^{1,8-11}

In the summer of 1994, CTA Inc., was awarded a contract from NASA to build the Clark spacecraft as part of the NASA Small Satellite Technology Initiative (SSTI) program. In the spring of 1995, Resonance Ltd. received a contract from North Carolina State University to design and build MicroMAPS (μ MAPS), a digital computer based gas filter correlation radiometer, to be flown on the Clark spacecraft. Because of budgetary overruns and schedule delays, the Clark mission was cancelled and the payload stored at NASA Goddard until August 2000. In 2002, the μ MAPS instrument was retrieved from storage and functional analyses determined that the instrument was still fully operational. Calculations and models were produced to determine the feasibility of integration of μ MAPS onto the Proteus,^{12,13} the highest flying private aircraft in the world. Integration

onto the Proteus, (Scaled Composites, Inc., Mojave, CA), was sought because it would operate at an altitude of about 16 km, allowing for detection of CO in the troposphere.

This paper examines the data from Proteus flights and outlines a method to extract surface temperature and CO volumetric mixing ratio. In section II, the μ MAPS instrument, its components, and their functions are described in detail. Section III describes the July 22, 2004 Proteus flight on which the retrieval analysis will focus, specifically presenting the flight path, and relevant instrument output. In section IV, the theoretical atmospheric and instrument models predicting the upwelling radiance seen by μ MAPS are discussed. Section V outlines the μ MAPS calibration procedure to determine a relationship between radiometric signal and instrument output followed by section VI which describes the calculations performed to relate the in flight instrument output to the atmospheric radiometric signal and CO mixing ratio.

II. The Aircraft and Instrument Description

The Proteus Aircraft

The Proteus Aircraft is owned and operated by Scaled Composites, Inc., an aerospace and specialty composites development company located in Mojave, CA. The Proteus is a twin turboprop high altitude multi-mission aircraft powered by Williams International FJ44-2E engines and has a unique tandem wing arrangement. The μ MAPS Instrument is designed to carry payloads of 2000 pounds at 55,000 feet and remain at altitude up to 14 hours.

MicroMAPS is a gas filter correlation radiometer (GFCR) that measures tropospheric CO in the 4.67 μ m band – the fundamental band of CO. The GFCR achieves high effective spectral resolution by internally comparing the incoming radiation to the incoming radiation as seen through a gas cell containing the gas of interest. As thermal radiation is emitted by the Earth and travels upward, it is attenuated by the atmospheric constituents. If it passes through a gas cell within the instrument, the energy due to that gas is removed. By comparing this signal to a signal through a clear channel that removes no energy, one can determine how much of the target gas is in the atmosphere below. This is the concept behind all GFCR instruments.

Figure 1 shows a functional schematic of μ MAPS and in the Proteus aircraft. Once the thermal radiation emitted by the earth's surface reaches the instrument, it travels through the various cells of a high speed chopper and through a filter specific to the wavenumber range of interest before finally being collected on the detector.

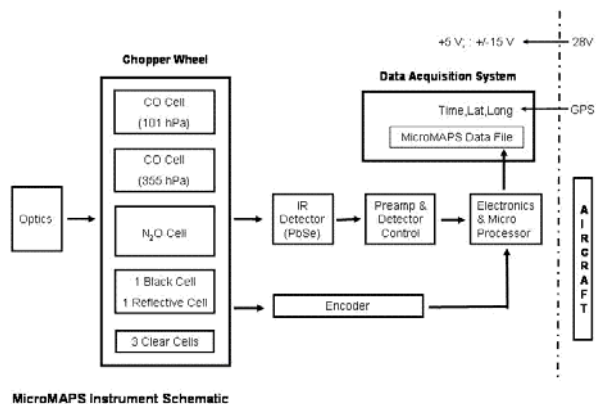


Figure 1. Functional schematic of the μ MAPS instrument onboard the Proteus aircraft. Not pictured is the bandpass filter which lies in between the chopper wheel and the IR detector.

Gas Cell Chopper

The μ MAPS chopper contains three sealed gas cells: CO at 76 Torr, CO at 266 Torr, and nitrous oxide (N_2O) at 115 Torr. The pressures were measured at a gas cell temperature of 296 K. Placed between these gas cells are evacuated cells (clear cells). One blackbody patch at the chopper temperature and one reflective patch for a cold reference are also present on the chopper wheel. All cells are one centimeter in length.

Upwelling energy passes through the cells as the chopper wheel rotates. Because of the high rotational speed of the wheel (2000 rpm), the radiation from the atmosphere at any point over the earth surface is assumed to pass through all of the aforementioned gas cells. As noted earlier, the gasses in these cells modify the energy in the upwelling radiation before the energy falls on the detector. The detector outputs as the earth and atmosphere are viewed through the various cells and digitized at the detector then electronically differenced by the μ MAPS internal computer to form difference signals. A mathematical description of these difference signals is given in the references.^{9,12} These difference signals are directly related to the correlation between the spectral lines of the gas in the gas cells and the spectral lines present in the incoming radiation. The difference signals form the basis for the measurement of CO in the atmosphere. The N_2O cell was originally incorporated for the purpose of filtering out cloud contaminated data in the satellite application. This has not been implemented in this aircraft application.

Bandpass Filter

The bandpass filter blocks out any incoming energy that is not in the CO 4.67 μ m spectral band. The bandpass filter data were recorded at 296 K and

linearly interpolated to achieve values at the necessary 0.01 cm^{-1} wavenumber increments. The filter temperature sensitive and spectral shifts occur at various temperatures. The shift is characterized by the following equation:

$$\lambda_2 = \lambda_1(1 - (2.0 \times 10^{-4})(T_2 - T_1)) \quad (1)$$

as determined from calibration testing. Figure 2 shows the transmission spectrum of the filter over the temperature range encountered during the flights.

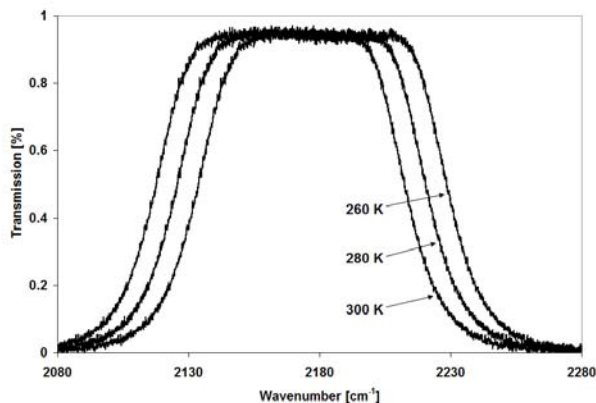


Figure 2. Predicted thermal shift of the bandpass filter from equation 1. The representative temperatures were chosen based on temperatures of the μ MAPS chopper during flights.

Data Acquisition System

The data acquisition and recording system is a PC-104 computer stack of four boards that is designed for high altitude flight application and nearly autonomous operation. Contained in an aluminum housing mounted to the half-inch thick aluminum base plate, the computer acquires and stores μ MAPS data, environmental sensor data, and aircraft-supplied navigation information (GPS latitude, longitude, and altitude). The data are time-tagged and output every three seconds. The data rate is controllable by the μ MAPS internal microprocessor. Currently, the data are averaged over approximately 100 revolutions of the chopper (corresponding to 3 seconds at 33.3 revolutions per second) and then output to the data acquisition system (PC-104).

III. Proteus Flight Data

Since its integration onto the Proteus,¹³ μ MAPS has participated in four scientific missions conducted in: North America (Intercontinental Chemical Transport Experiment-North America Science Team – INTEX-NA), Europe (Aerosol Direct Radiative Impact Experiment – ADRIEX and European AQUA Thermodynamic Experiment – EAQUATE), and Australia (Tropical Warm Pool Intercontinental Cloud Experiment – TWP-ICE). Of particular interest

is the July 22, 2004 flight during the INTEX-NA campaign during which portions of the flight path successfully overflew the DC-8 aircraft (Differential Absorption CO Measurement – DACOM instrument) and underflew the Aqua satellite (Atmospheric Infrared Sounder – AIRS instrument) so reliable CO comparisons could be made to validate the μ MAPS retrieval. The July 22nd flight path of Proteus and DC-8 along with the AIRS swath on the AQUA satellite are shown in Figure 3.

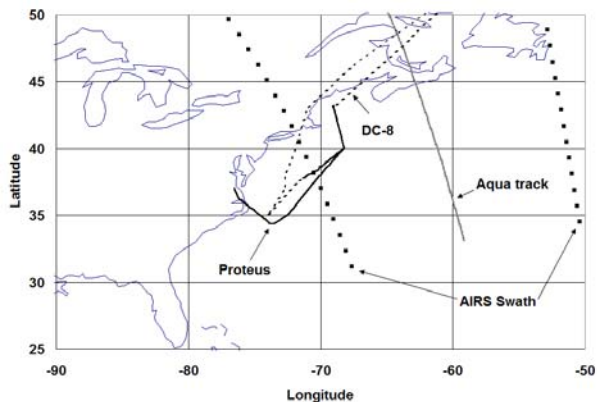


Figure 3. Proteus flight path during on July 22, 2004 as part of the INTEX-NA campaign. The flight path of the DC-8 aircraft and Aqua satellite are also shown. These platforms house other CO measuring instruments that will be used for μ MAPS validation, DACOM (DC-8) and AIRS (Aqua),

The μ MAPS data stream outputs flight information useful for calibration and sensitivity analysis along with navigation data, temperature of the various components of the instrument, and signals detected through the cells in the chopper. Figure 4 show the μ MAPS output through various gas channels during the July 22nd flight. These specific signals are of interest for surface temperature and CO retrieval which will become apparent in subsequent sections of this paper. These signals represent the detector signal registered from three different channels: the cold reference, the high pressure CO cell, and a vacuum cell. The cold reference allows for the amount of scattered radiation from various other optics of the μ MAPS instrument to be taken into account. Subtracting this signal from the signal seen through the clear cells gives a value that is proportional to the upwelling radiance. Subsequent differencing of this signal with the signal seen through the high pressure CO cell determines the value that is proportional to the CO in the upwelling radiance. These difference signals as a function of the μ MAPS chopper temperature are shown in Figure 5. For simplicity in this work, we will refer to the two signals shown in Figure 5 as S_f and ΔS_f where $S_f =$

(Average of the clear cell Signals) – (Cold reference signal) and $\Delta S_f = S_f - (\text{CO 266 signal})$ and the subscript “f” is used to designate these difference signals as those from the flights.

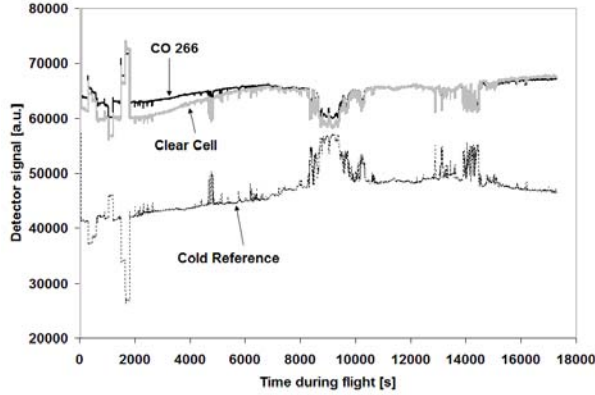


Figure 4. Raw signal from various channels during flight. Note how the cold reference mirrors the other signals. This quantifies the amount of scattered radiation from other parts of the instrument.

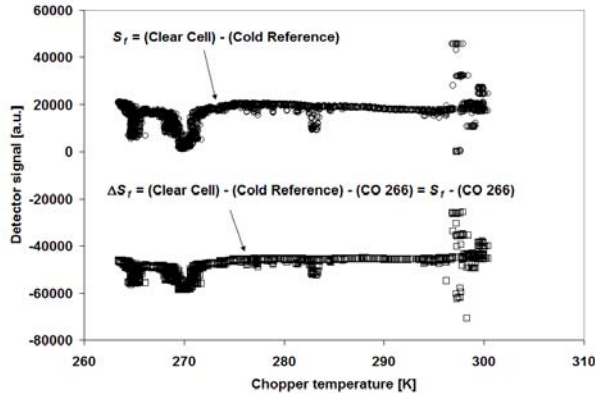


Figure 5. Useful combinations of the signals shown in Figure 4. These signals, S_f and ΔS_f , are critical for surface temperature and CO retrieval.

IV. Atmospheric and Instrument Model

In this work we considered only thermal radiation emitted by the earth as modified by the absorption and emission of the atmosphere. At these wavelengths reflected sunlight accounts for less than ten percent of the upwelling radiation.¹⁴ The most significant source of radiation is the earth’s surface. As this radiation travels upward, it is absorbed by the various constituents in the atmosphere. These gasses, in addition to absorbing the upwelling radiance, also emit radiation thereby contributing to the radiation detected by the instrument.

The monochromatic upwelling radiation at the instrument, $L(\nu)$, includes not only the radiation from the Earth’s surface, but also the absorption and emission from gasses in the atmosphere. $L(\nu)$ is

calculated using the Line By Line Radiative Transfer Model (LBLRTM). LBLRTM is a product of Atmospheric and Environmental Research, Incorporated (AER), and is considered the industry standard for accurate atmospheric modeling. LBLRTM is a FORTRAN-based program that extracts data from the HITRAN 1992 database and it is used to predict and simulate the transmission and emission of radiation in the atmosphere.¹⁵ LBLTRM is used with input parameters appropriate to the μ MAPS flights to generate a range of atmospheric radiation models. Inputs for LBLRTM include: specific molecules to consider (i.e. which absorption characteristics to incorporate from the HITRAN 1992 database), wavenumber range of interest, surface temperature, surface emissivity, and altitude of nadir viewing. In addition, LBLRTM allows for a custom defined atmosphere by defining pressure, temperature, and molecular number density in user defined atmospheric layers at different altitudes.

Incident radiation was modeled in the wavenumber range of 2080cm^{-1} - 2280cm^{-1} in 0.01cm^{-1} increments. The flight altitude for μ MAPS on Proteus flights is 15 km, or about 50,000 ft above the earth. The earth was modeled at seven different surface temperatures (280 K – 310 K) and a surface emissivity of 0.98 is assumed. LBLRTM was run with two different atmospheres. First, LBLRTM is run to model the five major absorbing gasses in the atmosphere in the spectrum of interest (H_2O , CO_2 , O_3 , N_2O , and CO).¹⁴ In these calculations, a 1976 standard atmosphere was assumed.¹⁶ Then, to examine the relative effect of CO in this range, LBLRTM is run again with only CO in the modeled atmosphere. In these calculations, a custom atmosphere is defined in the LBLRTM input using altitude specific pressures and temperatures from the 1976 standard atmosphere in each layer, and specifying CO as the only molecule present. The amount of CO in each layer was varied to change the total column density. A uniformly mixed column was implemented, and calculations with CO spanning 70 – 150 ppbv were performed.

The instrument model describes the effects of the instrument on the upwelling radiation. The effects of the gas cells and the bandpass filter must be taken into account. HITRANPC was used to model the transmission of the gas cells. For this application, HITRANPC, using the HITRAN 1992 database, allows the user to input the gas through which the energy will be transmitted, the partial pressure of the gas in the cell, the temperature in which the gas cell is maintained, and the size of the gas cell. The pressures of the sealed cells are temperature sensitive and vary in accordance with Boyle’s Law. One assumption used in the model of the instrument is the temperature of the gas cell is equivalent to the temperature of the μ MAPS bandpass

filter. The temperature of the gas cell wheel, or chopper, is output in the μ MAPS data stream. This, along with varying temperatures of the earth in LBLRTM, allowed for the theoretical model to be calculated at varying source temperatures and varying gas cell and bandpass filter temperatures. The transmissions through the vacuum cells are assumed as unity.

The upwelling radiance from the atmospheric model is transmitted through the gas and vacuum cells and the bandpass filter and the result is integrated over the wavenumber spectrum. The signal through the vacuum cell is of interest when using the LBLRTM atmosphere with the five major absorbing gasses, and the difference signal between the vacuum cell and high pressure CO cell is important when modeling a CO only atmosphere. A trapezoidal integration scheme was used to numerically integrate of the spectrum. These calculations were performed several times using the earth source and instrument temperatures that were representative of the temperatures encountered during the Proteus flights. The theoretical radiometric signals described above can be mathematically expressed as:

$$L_f(T_e, T_i) = \int_{\nu} L_5(\nu, T_e) \tau_{bpf}(\nu, T_i) \tau_{vac}(\nu, T_i) d\nu \quad (2)$$

$$\Delta L_f(T_e, T_i, VMR) = \int_{\nu} L_{CO}(\nu, T_e, VMR) \tau_{bpf}(\nu, T_i) [\tau_{vac}(\nu, T_i) - \tau_{CO266}(\nu, T_i)] d\nu \quad (3)$$

where L represents the radiances as calculated by LBLRTM, ν is the wavenumber, T is the temperature of the earth's surface or the instrument, τ is the transmission of a μ MAPS component, and VMR is the CO volumetric mixing ratio used when defining the CO atmosphere. The subscripts of L refer to the type of atmosphere used, where "5" represents the atmosphere using the major absorbing gasses and "CO" refers to a CO only atmosphere. The subscripts of the transmission terms refer to the bandpass filter, vacuum cell, and high pressure CO cell. The subscript "f" is used to designate these calculations (which model flight conditions) from other theoretical calculations performed to model calibration conditions. These other calculations will be discussed later.

Results of the theoretical flight calculations – L_f and ΔL_f – are shown in Figure 6. The curves represent the radiometric signals detected by μ MAPS with the two different atmospheres described above at various instrument temperatures. The CO atmosphere shown was defined with a uniformly mixed vertical column with 110 ppbv. The figure shows two representative earth surface temperatures, 280 K and 300 K. These specific calculations are crucial to the surface temperature and CO retrievals. These curves

are related to the data shown in Figure 5, where $L_f(T_e, T_i)$ is related to the signal S_f , and $\Delta L_f(T_e, T_i)$ is related to the signal ΔS_f . To proceed with retrievals, this relationship must be determined via instrument calibration.

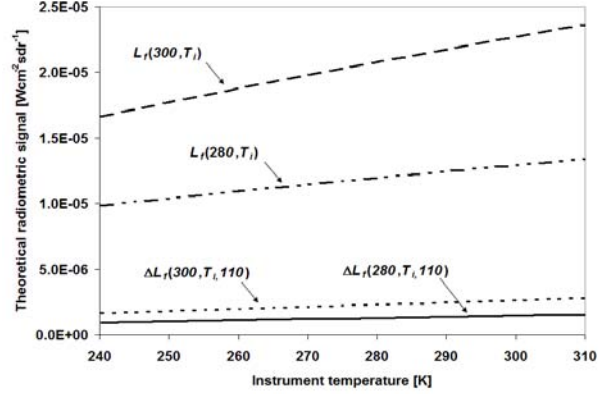


Figure 6. The predicted radiance for various instrument temperatures during flight as calculated from equations 2 and 3. Each equation is calculated at 2 blackbody temperatures.

V. Instrument Calibration

The μ MAPS instrument calibration was carried out at Resonance Ltd. in Barrie, Ontario, Canada, where μ MAPS was designed and constructed, in early June 2005. The equipment was the same as those used previously for the original calibration for the Clark spacecraft mission. The goal of the calibration was to determine the μ MAPS signal response to blackbody target temperature for a range of μ MAPS instrument temperatures in order to produce a signal to surface temperature ratio. The cooling of the instrument was controlled with a varying mass of dry ice, and the range of instrument temperatures was chosen to match instrument temperatures reported by μ MAPS during the Proteus flights in July – September 2004. The external blackbody source was temperature controlled so that at chosen μ MAPS instrument temperatures, the signal could be determined for a range of blackbody temperatures. The range of blackbody temperatures were chosen to match earth surface temperatures measured by NOAA buoy data during the Proteus flights. To simulate a CO rich atmosphere, a sealed CO gas cell was placed in the field of view of the μ MAPS detector between the nacelle window and the external black body target. The CO

gas cell was a refillable glass cell that was 31 mm in internal length and 50 mm in diameter pressurized to 250 Torr. The cell was filled with a mixture of 12.46 % CO in N₂. Calibration data were taken with and without the sealed gas cell in the field of view.

Selected results of the μ MAPS calibration are shown in Figures 7 and 8. In the actual data retrieval process, more calibration data was utilized, but for clarity in presentation, only a few data points are presented in the figures. Figure 7 shows the difference signal between the clear cells and the cold reference when the gas cell is not in the field of view. Paralleling the previous discussion, this signal is designated as S_c , where the subscript “c” refers to calibration. These data show how S_c varies with chopper temperature and external blackbody temperature. Similarly, in Figure 8, ΔS_c is presented, which is the difference signal between S_c and the CO 266 signal. This calculation is the same as that used to determine ΔS_f . Comparing the similarly calculated signals in Figure 5 to Figures 7 and 8 a likeness in sign and magnitude is observed, validating our calibration conditions and assumptions.

The theoretical radiative transfer calculations to compute the radiometric signals during calibration conditions were similar to those outlined in section IV. However, due to the calibration set up, the calculations were simplified. The blackbody target was modeled using Planck’s function, and in the case when the external CO gas cell was not in the field of view, the blackbody radiation was assumed to be unperturbed before entering the instrument (i.e. no atmosphere was modeled). For the situation with the external cell, HITRAN PC was used to model the transmission of the CO gas cell and the blackbody radiation was passed through this “CO atmosphere” before the instrument model. The model of the external cell assumed the cell was at a constant temperature, 298 K, which was monitored during calibration. These theoretical radiometric signals can be mathematically expressed as:

$$L_c(T_e, T_i) = \int_{\nu} L_p(\nu, T_e) \tau_{bpf}(\nu, T_i) \tau_{vac}(\nu, T_i) d\nu \quad (4)$$

$$\Delta L_c(T_e, T_i) = \int_{\nu} L_p(\nu, T_e) \tau_{ext}(\nu) \tau_{bpf}(\nu, T_i) [\tau_{vac}(\nu, T_i) - \tau_{CO266}(\nu, T_i)] d\nu \quad (5)$$

where the subscripts “p” and “ext” refer to Planck’s function and the external CO gas cell. Results of these calculations are presented in Figure 9. Both the theoretical signals – L_c and ΔL_c – and the measured signals during calibration – S_c and ΔS_c – are relatively flat over the instrument temperature studied, and both demonstrate an increase with increasing blackbody temperatures. ΔS_c in Figure 8 decreases with increasing blackbody temperature which is not consistent with our

model of ΔL_c shown in Figure 6. However, since both S_f and S_c are negative, the increase in signal with increasing blackbody temperature relationship is still maintained during CO retrieval. This will become more apparent in the next section with the data retrieval discussion.

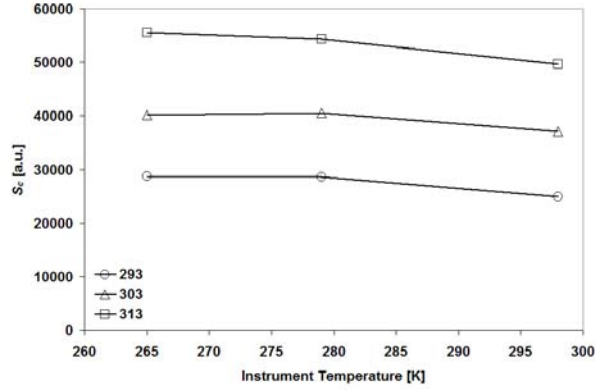


Figure 7. S_c vs. instrument temperature for 3 different blackbody temperatures calculated from calibration data. S_c is calculated similar to S_f .

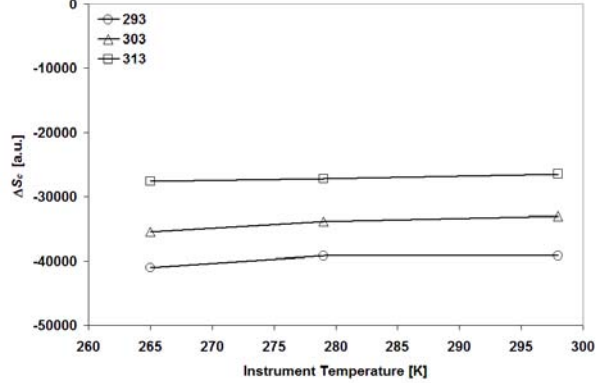


Figure 8. ΔS_c vs. instrument temperature for 3 different blackbody temperatures calculated from calibration data. ΔS_c is calculated similar to ΔS_f .

VI. Data Retrieval

Retrieval of earth surface temperature and CO MIXING RATIO was pursued by establishing relationships between the theoretical and measured signals between the calibration and flight.

Surface Temperature

The signal detected by μ MAPS during the flight was related to the radiance emitted from the earth

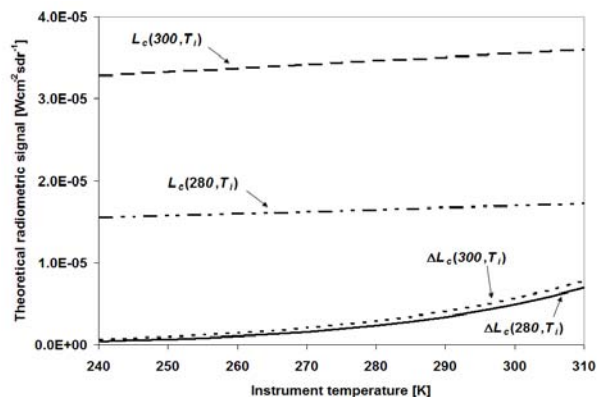


Figure 9. The predicted radiance for various instrument temperatures during calibration as calculated from equations 4 and 5. Each equation is calculated at 2 blackbody temperatures.

surface, which is dependent on the surface temperature. Since all the molecules in the atmosphere affect this upwelling radiation, L_f needs to be related to S_f to infer the surface temperature during flights. To accomplish this, a temperature dependent proportionality constant was calculated from the calibration data. This constant was then multiplied by the flight model to predict the signal during flight at a given instrument temperature and source temperature. This is mathematically expressed as:

$$S_{predicted} = \frac{S_c}{L_c(T_e, T_i)} L_f(T_e, T_i) \quad (6)$$

where the aforementioned proportionality constant is $S_c/L_c(T_e, T_i)$. $S_{predicted}$ was calculated with the instrument temperature reported in flight and for a range of source temperatures. The signal from flight, S_c , was then matched to $S_{predicted}$ and the T_e at which they corresponded was backed out, linearly interpolating between calculated points. The surface temperature determined by μ MAPS is compared to the surface temperature reported by AIRS and NOAA buoy data in Table 1. The surface temperature inferred from μ MAPS data agrees with previously reported values to within 0.1 %. Accurate surface temperature retrieval is necessary to successfully determine CO mixing ratios.

Table 1. July 22nd Surface Temperature Comparison

Instrument	Latitude	Longitude	T_e [K]
AIRS	39.58	-68.91	292.9
μ MAPS	39.58	-68.75	293.1
AIRS	40.24	-68.23	293.4
μ MAPS	40.24	-68.27	293.6
NOAA buoy	41.26	-69.29	290.5
μ MAPS	41.47	-68.57	290.8

CO Mixing Ratio

In a manner similar to the procedure for surface temperature retrieval, CO mixing ratios were inferred. Since T_e has already been determined, that information was used in conjunction with T_i to calculate ΔL_c and ΔL_f as shown in equation 7.

$$\Delta S_{predicted} = \frac{\Delta S_c}{\Delta L_c(T_e, T_i)} \Delta L_f(T_e, T_i, VMR) \quad (7)$$

ΔL_f was calculated for a wide range of CO mixing ratios. $\Delta S_{predicted}$ and ΔS_f were then matched at the corresponding CO mixing ratio by linearly interpolation, which is a valid assumption in the range of CO mixing ratios appropriate for CO.¹⁴ The results of the CO retrieval are shown in Figure 10.

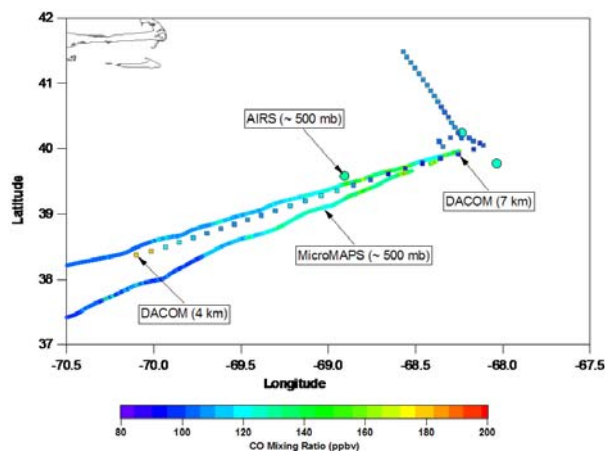


Figure 10. CO mixing ratio measurements on July 22nd. Measurements during the μ MAPS are shown for the entire flight. Selected AIRS and DACOM measurements are presented for comparison.

For the majority of the flight, μ MAPS measured 110 – 150 ppbv CO. AIRS and μ MAPS reported about 130 ppbv CO when in the same vicinity. DACOM measurements were lower than μ MAPS for the majority of the flight. This could be a result of DACOM flying at a lower altitude than μ MAPS, and below that peak concentration of CO in the standard atmosphere, about 9 km.^{13,16} In general, the close agreement of μ MAPS to other instruments validates the retrieval process and confirms that μ MAPS is an accurate radiometer for CO measurements.

VI. Conclusions

This paper presented the temperature and CO mixing ratio retrieval algorithm for the μ MAPS instrument, a light weight, cost efficient CO GFCR. Flight data from the July 22, 2004 Proteus flight during the INTEX-NA campaign were presented. The instrument calibration was outlined, and calibration data were reported that simulated the July 22nd flight.

Calculations that modeled both flight and calibration conditions were explained. The temperature and retrieval algorithm using flight, calibration, and model data was outlined. Sample surface temperature and CO mixing ratio data were presented and compared to other platforms.

The close agreement of μ MAPS measurements to other surface temperature and CO mixing ratio data suggests that μ MAPS is an accurate radiometer. For future work and more accurate statistical comparisons, the μ MAPS Averaging Kernel must be applied to data to take into account the vertical distribution of CO in the atmosphere to correct for instrument sensitivity. Data filtering should also be implemented to correct for cloud cover and aircraft roll so that all flights, so that accurate CO information can be measured during any flight condition.

Acknowledgements

This work would not have been possible without: Gao Chen for help with the presentation of the data, Pam Norris for continued encouragement and academic advice, Don Oliver for help with instrument calibration, Bill Morrow for insightful discussions, and NASA and VSGC for financial support.

References

- 1 V. S. Connors, *et al.*, Journal of Geophysical Research **104**, 21455 (1999).
- 2 J. A. Logan, *et al.*, Journal of Geophysical Research **86**, 7210 (1981).
- 3 O. Badr and S. Probert, Applied Energy **49**, 99 (1994).
- 4 N. Sze, Science **195**, 673 (1977).
- 5 M. V. Migeotte, Physical Review **75**, 1108 (1949).
- 6 O. Badr and S. Probert, Applied Energy **49**, 145 (1994).
- 7 C. Ludwig, *et al.*, Applied Optics **13**, 1494 (1974).
- 8 H. Reichle, *et al.*, Journal of Geophysical Research **95**, 9845 (1990).
- 9 H. Reichle, *et al.*, Journal of Geophysical Research **91**, 10865 (1986).
- 10 H. Reichle, *et al.*, Journal of Geophysical Research **104**, 21443 (1999).
- 11 H. Wallio, *et al.*, Applied Optics **21**, 749 (1983).
- 12 P. E. Hopkins and R. J. Ribando, *Proceedings of the Virginia Space Grant Consortium Student Research Conference*, Hampton, VA (2004).
- 13 P. E. Hopkins, *et al.*, *Proceedings of the Virginia Space Grant Consortium Student Research Conference*, Hampton, VA (2005).

- 14 H. G. Reichle, *et al.*, Applied Optics **28**, 2104 (1989).
- 15 L. S. Rothman, *et al.*, Journal of Quantitative Spectroscopy and Radiative Transfer **48**, 469 (1992).
- 16 National Oceanic and Atmospheric Administration (NOAA), U. S. Standard Atmosphere, 1976, U. S. Government Print Office, Washington, D. C. (1976).